Quality Improvement Study

Medicine®

OPEN

A novel iterative modified bicubic interpolation method enables high-contrast and high-resolution image generation for F-18 FDG-PET

Atsutaka Okizaki, MD, PhD*, Michihiro Nakayama, MD, PhD, Kaori Nakajima, MD, Koji Takahashi, MD, PhD

Abstract

Positron emission tomography (PET) has become a useful and important technique in oncology. However, spatial resolution of PET is not high; therefore, small abnormalities can sometimes be overlooked with PET. To address this problem, we devised a novel algorithm, iterative modified bicubic interpolation method (IMBIM). IMBIM generates high resolution and -contrast image. The purpose of this study was to investigate the utility of IMBIM for clinical FDG positron emission tomography/X-ray computed tomography (PET/CT) imaging.

We evaluated PET images from 1435 patients with malignant tumor and compared the contrast (uptake ratio of abnormal lesions to background) in high resolution image with the standard bicubic interpolation method (SBIM) and IMBIM. In addition to the contrast analysis, 340 out of 1435 patients were selected for visual evaluation by nuclear medicine physicians to investigate lesion detectability. Abnormal uptakes on the images were categorized as either absolutely abnormal or equivocal finding.

The average of contrast with IMBIM was significantly higher than that with SBIM ($P < .001$). The improvements were prominent with large matrix sizes and small lesions. SBIM images showed abnormalities in 198 of 340 lesions (58.2%), while IMBIM indicated abnormalities in 312 (91.8%). There was statistically significant improvement in lesion detectability with IMBIM ($P < .001$).

In conclusion, IMBIM generates high-resolution images with improved contrast and, therefore, may facilitate more accurate diagnoses in clinical practice.

Abbreviations: F-18 FDG = 2-[18F]fluoro-2-deoxyglucose, IMBIM = iterative modified bicubic interpolation method, maxSUV = maximum standardized uptake value, MRI = magnetic resonance imaging, PET = positron emission tomography, PET/CT = positron emission tomography/X-ray computed tomography, SBIM = standard bicubic interpolation method, SUV = standardized uptake value.

Keywords: bicubic method, FDG PET, high-resolution image, malignant tumor

1. Introduction

Positron emission tomography/X-ray computed tomography (PET/CT) performed with 2-[18F]fluoro-2-deoxyglucose (F-18 FDG) has become a useful and important technique in oncology.[1,2] F-18-FDG PET/CT is recommended for preoperative staging,[3,4] evaluation of recurrence,[5] and assessments of therapeutic response.[6] However, spatial resolution of PET is generally from 3 to 4 mm, which is lower than that of CT or magnetic resonance imaging (MRI). Therefore, small abnormalities can sometimes be overlooked with PET. Biases, such as underestimation of tracer uptake, in small structures associated with resolution blurring are called "partial volume effect."[7] Some authors have reported on partial volume correction using CT or MRI.[8] In these cases, both PET and anatomic images are necessary to perform the correction. Another correction approach is deconvolution of point spread function.[9] Although these attempts can be very useful, they do not increase image resolution.

Recently, PET scanners with semiconductor detectors have been shown to facilitate acquisition of high-resolution and -quality images. Semiconductor PET scanners are able to directly convert γ-rays into signal without scintillator material,[10,11] enabling acquisition of high-resolution spatial and energy images. Shiga et al[12] reported that semiconductor PET scanning enabled better identification of intratumoral inhomogeneity. However, semiconductor PET scanners are only available at some research centers because they are very expensive.

Generally, interpolation methods (e.g., bilinear and bicubic) are frequently used to generate high-resolution images.[13] These methods estimate interpolated data calculated by weighted surrounding pixel values on X and Y axes separately. Creating a high-resolution image from low resolution images requires an increase in the total number of pixels; therefore, this gap must be filled with the interpolated data. In this case, the peak pixel value in the image remains unchanged. To address these problems, we devised a novel algorithm for creating high-resolution image

Editor: Bernhard Schaller.

Disclosure: IMBIM method has a patent in USA (US 9159120 B2) and in Japan (No. 5863554). One of the authors of this study (Atsutaka Okizaki) is a coinventor on this patent. No other potential conflict of interest relevant to this article was reported.

The authors report no conflicts of interest.

Department of Radiology, Asahikawa Medical University, Asahikawa, Japan.

* Correspondence: Atsutaka Okizaki, Department of Radiology, Asahikawa Medical University, 2-1-1-1 Midorigaoka-higashi, Asahikawa 078-8510, Japan (e-mail: okizaki@asahikawa-med.ac.jp).

Medicine (2017) 96:52(e9472)

Received: 2 October 2017 / Received in final form: 23 November 2017 / Accepted: 5 December 2017

http://dx.doi.org/10.1097/MD.0000000000009472

data, called the iterative modified bicubic interpolation method (IMBIM). It is important to achieve high resolution and -contrast image data by development of new software, and not hardware, for cost-effectiveness. Therefore, the objective of this study was to investigate the utility of IMBIM for clinical FDG PET/CT imaging.

2. Methods

2.1. Theory

To simplify, consider an example wherein only the center of a pixel has a high uptake value, while the surrounding pixels have no uptake value (Fig. 1A-1). Figure 1A-2 shows the count profile curve of Fig. 1A-1. The matrix size is 5×5 in this example, and a pixel value is expressed as the brightness. By increasing the resolution to 15×5 with standard bicubic interpolation method (SBIM), a pixel on the original image corresponds to 3×3 pixels on the higher resolution image (Fig. 1B-1; count profile curve, Fig. 1B-2). The central pixel on the original image and the central 3×3 pixels on the high-resolution image (inside red square, Fig. 1A, B) both have the same maximum value (hatched area, Fig. 1A, B), but the value of the surrounding pixels on the high-resolution image, which are interpolated with SBIM, are smaller than that of the central pixel on the original image due to effects from the value of outer pixels (dotted area, Fig. 1B). The total amount of brightness inside the square area on high-resolution images should be the same as in the original image; however, they are different. We hypothesized that this difference may be minimized by the addition of a correction value to the pixel value on the original image (Fig. 1C), which is calculated with the following formula:

$$\text{Correction value} = (\text{central pixel value on original}) - (\text{average pixel value inside red square on high} - \text{resolution}) \quad (1)$$

Procedures with IMBIM are more complicated in clinical practice because each pixel value may interact with adjacent pixels. A single procedure may not be enough, however, the difference between a pixel value on the original image and average of pixel values on high-resolution images will be reduced by repeating this procedure. The same principle should be true for situations in which a low pixel value is surrounded by high pixel values. Furthermore, SBIM data are calculated based on X and Y directions; thus, the pixel values change depending on the direction of the subject. Therefore, we used weight parameters derived from the distance between each pixel in IMBIM, not separate X and Y directions, because the values should not change with the subject's direction.

2.2. Subjects

Between January 2015 and July 2016, 2017 serial adult patients suspected of having malignant tumors were enrolled in our study. Of them, 582 patients were excluded because they had no abnormal uptake and did not have a diagnosis of malignant disease. Finally, 1435 patients (mean age ± standard deviation, 67.0 years ± 12.0; age range, 21–90 years; 805 men and 630

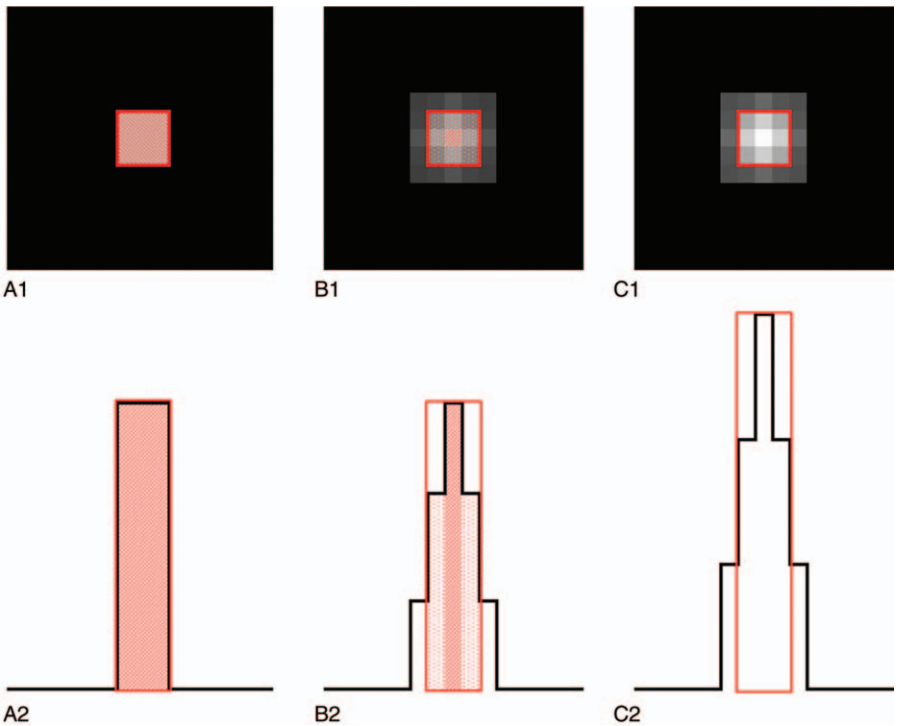

Figure 1. (A-1) Original image example; (A-2) count profile of (A-1). (B-1) and (C-1) are high-resolution images generated by SBIM and IMBIM, respectively; (B-2) and (C-2) are their respective count profiles. The amount of signal information in the central pixel on the original image (inside red square in A and B) decreased to 76.8% in this case. However, using IMBIM, 96.6% of the signal information was reserved (inside red square in C). Furthermore, the maximum signal in (A) and (B) are the same, while in (C), it is higher than the original. Therefore, IMBIM generated a high-contrast and -resolution image. IMBIM = iterative modified bicubic interpolation method, SBIM = standard bicubic interpolation method.

women) with malignant tumor were enrolled. We measured the maximum standardized uptake value (maxSUV) of abnormal lesions from each patient by F-18 FDG PET scan and their shortest diameter via CT. Standardized uptake value (SUV) was calculated as follows:

$$\mathrm{SUV} = \frac{[\text{decay} - \text{corrected activity (kBq)}/\text{tissue volume (mL)}]}{[\text{injected FDG activity (kBq)}/\text{body weight (g)}]} \quad (2)$$

The study protocol was approved by our institutional research ethics committee in accordance with the principles of the Declaration of Helsinki (approval number: 16086). Informed consent was not deemed necessary by the ethics committees because the study was retrospective and noninvasive.

2.3. FDG PET/CT scanning

Each patient was intravenously injected with 185 MBq of 18F-FDG as a bolus, and PET/CT images were acquired according to standard protocols using a PET/CT device (Discovery VCT, GE, Japan). Acquisition began 60 minutes after 18F-FDG injection, and all patients fasted for 6 hours before injection. A non-enhanced, low-dose CT scan was acquired for attenuation correction at 120 keV with auto-mA (20–100) for attenuation correction and anatomic localization. Data were reconstructed with a standard filter into transaxial slices with a 50-cm field of view, 512×512 matrix size (pixel size, 0.98 mm), and slice thickness of 3.3 mm. The size of lesions was obtained with CT. After the CT scan, PET images were obtained in 3 dimensions. The acquisition time was 3 min/bed, and the scan had 8 bed positions (head to mid thighs) with a 60-cm field of view. Attenuation correction was based on the CT scan. PET data were reconstructed into transaxial slices with a matrix size of 128×128 (pixel size, 4.69 mm) and a slice thickness of 3.3 mm using iterative 3-dimensional ordered subset expectation minimization (2 iterations, 14 subsets). All images complied with Digital Imaging and Communication in Medicine format.

2.4. IMBIM algorithm

First, a high-resolution image (High-Image) was made from the original image with the modified SBIM. While SBIM weight parameters are calculated in X and Y directions separately, our IMBIM uses weight parameters derived from the distance between the interpolated data and each surrounding pixel on the XY plane. The value of the new pixel was then acquired using the following equation:

$$X_{\mathrm{new}} = \frac{\sum_{k=1}^{m}(x_k \times a_k)}{\sum_{k=1}^{m}(a_k)} \quad (3)$$

where m is the number of original pixels positioned within a predesignated distance around the new pixel, X_{new} is the value of the new pixel, x_k is the pixel value of a k-th original pixel positioned within a predesignated distance around the new pixel, and a_k is a weighting value set in accordance with the distance between the k-th and new pixel. Weighting value a_k is given by the following formula:

$$f(x) = \frac{\mathrm{sinPI}(t)}{\mathrm{PI}(t)} \quad (4)$$

where, t is the distance from the new pixel to each original pixel, and PI is circular constant.

Second, an original resolution image (Low-Image) was made from the High-Image, wherein each pixel value is an average of the corresponding pixel values on the High-Image. Then, the original image and Low-Image were compared, and correction values determined for each pixel by subtracting the pixel value on the Low-Image by that of the original data. The corrected Low-Image was then created by adding each pixel value on the original image to the correction value. Next, a high-resolution image was created from the corrected Low-Image. The entire procedure was continued until all correction values were small enough (<10%) or the repeat times reached a prescribed number (3 times). Finally, the high-resolution image was generated.

2.5. Evaluation of contrast

Comparisons of contrast in 386×386, 640×640, 896×896, 1152×1152, and 1408×1408 pixel areas generated by SBIM and IMBIM were performed on 1435 lesions. Each pixel area was categorized into 4 groups with SUV as follows: other lesions or physiological uptake (>maxSUV in lesion); tumor uptake (50–100% maxSUV in lesion); background (0.2–50% maxSUV in lesion); outside the body (<0.2). Specifically, contrast was calculated as follows:

$$\text{Contrast} = \frac{(\text{maxSUV in lesion})}{(\text{average SUV of background})} \quad (5)$$

Moreover, the rate of contrast change was calculated as:

$$\text{Rate of Contrast Change} = \frac{(\text{contrast in high} - \text{resolution})}{(\text{contrast of original})} \quad (6)$$

2.6. Evaluation of visual score

In addition to contrast analysis, 340 out of 1435 patients, who had abnormal uptake of malignant tumor confirmed by follow-up PET/CT or CT scan, were selected for visual evaluation. Visual evaluation of F-18 FDG PET/CT scans were made in a randomized order and independently by 2 nuclear medicine physicians with high-resolution images (386×386) generated by SBIM and IMBIM. Abnormal uptake on an image was categorized as either an absolutely abnormal or equivocal finding. When the interpretations were different, the disagreements were resolved by consensus after discussion. The follow-up scan was performed from 3 to 6 months later.

2.7. Statistical analysis

Wilcoxon matched-pairs signed rank test was used for evaluation of the contrast difference in each image generated by SBIM and IMBIM. Spearman's rank correlation coefficient was used to investigate the relationship between the rate of contrast change and matrix size, and the rate of contrast change versus the shortest lesion diameter. McNemar test was used to examine whether the ratio between absolutely abnormal and equivocal findings were changed or not by using IMBIM compared with SBIM. A $P < .05$ was considered significant. All statistical analyses were performed with JMP (version 12, SAS Institute Japan, Japan).

3. Results

The average contrasts in all resolution images assessed with SBIM were 6.98, while that of 386×386, 640×640, 896×896,

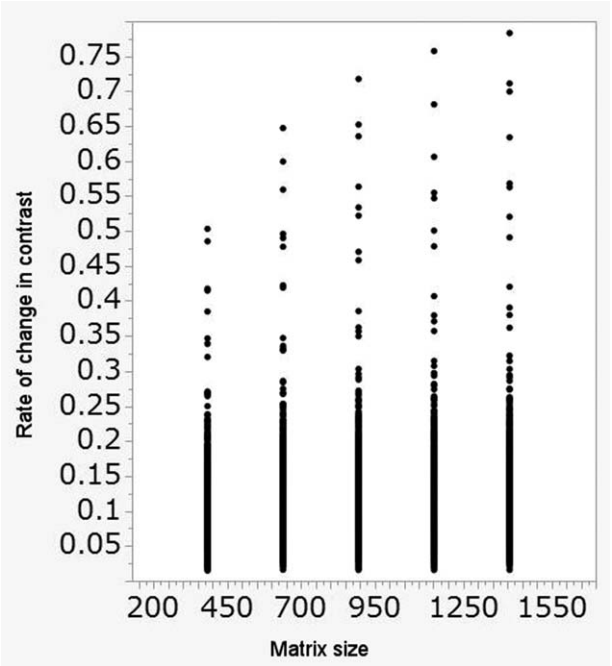

Figure 2. Scatter plot of the rate of contrast change versus generated matrix size. These variables showed a significantly positive correlation ($P < .001$).

1152 × 1152, and 1408 × 1408 images with IMBIM were 7.72, 7.80, 7.83, 7.84, and 7.85, respectively. Hence, there were statistically significant differences between SBIM and IMBIM values at all resolutions ($P < .001$ in all groups). Moreover, a positive correlation was observed between the rate of contrast change and matrix size (Fig. 2, $P < .001$). On the other hand, a negative correlation was observed between the rate of contrast change and lesion size in all of high-resolution images with IMBIM (Fig. 3A–E, $P < .001$ in all groups). The contrast change was not observed in all of high-resolution images with SBIM.

Figure 4 shows an example of 18F-FDG PET images of the neck. High-resolution images were generated by SBIM (Fig. 4B) and IMBIM (Fig. 4C). In this study, SBIM images showed abnormalities in 198 of 340 lesions (58.2%), while IMBIM images indicated abnormalities in 312 (91.8%). There was statistically significant improvement in lesion detectability with IMBIM ($P < .001$). Any false-positive lesion due to IMBIM was not found in this study.

4. Discussion

IMBIM generated high-resolution images with improved contrast. The improvement in contrast was more prominent with as the matrix size increased and lesion size. Moreover, substantial equivocal findings with SBIM were changed to absolutely abnormal using IMBIM clinically. Several studies have shown that partial volume correction algorithms and high-resolution hardware are useful for accurate diagnoses because they improve the contrast between abnormal lesions and peripheral physiological uptake. Takei et al[14] reported that semiconductor PET scanning is useful especially for small lesions (≤10 mm). The results of our study agree with previous reports. Herein, 50% of the maxSUV was used as a threshold between physiological uptake and tumor, similar to Usmanij et al.[15] Some reports have used anywhere from 40% to 60% of the maxSUV or gradient-based methods for the threshold,[16–19] but there is not yet a consensus. Therefore, the threshold setting might have slightly affected the current results. However, it does not influence our conclusions because the imaging contrast was so obviously improved.

In principle, minimization of partial volume effect in medical images is desirable because it obscures the image and consequently, may hinder an accurate diagnosis. Therefore, higher resolution medical imaging systems are being developed. Some authors reported the usefulness of high-resolution CT for accurate diagnosis of lung disease nearly 20 years ago.[20,21] IMBIM may be useful not only for PET, but also for other medical imaging techniques, such as CT, MRI, ultrasound, and

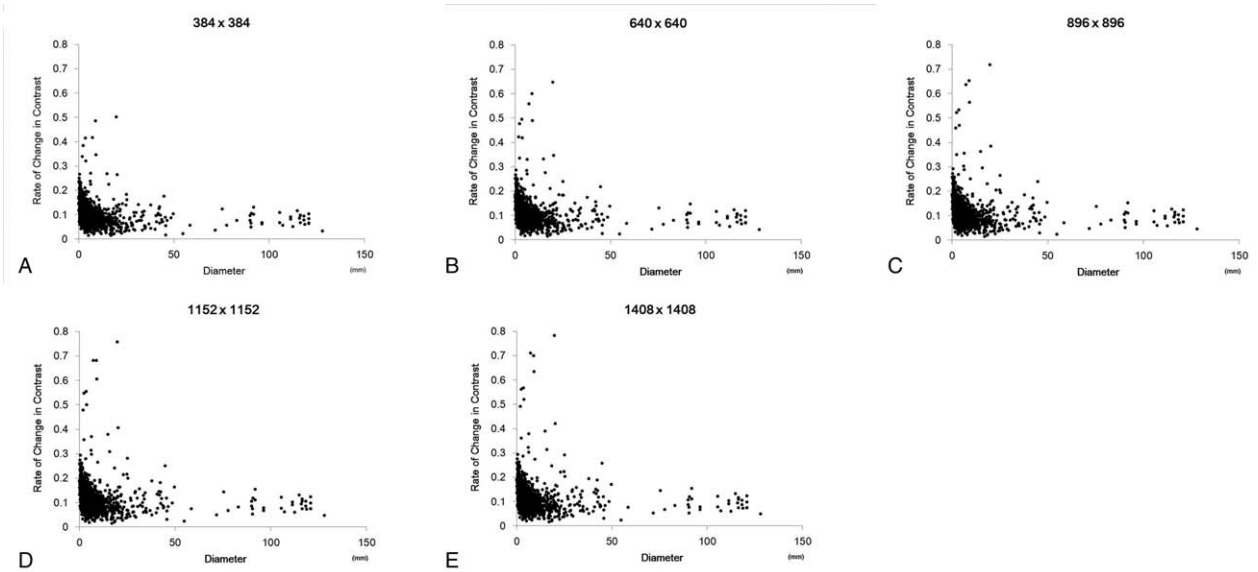

Figure 3. Scatter plots of the rate of contrast change and lesion diameter in 384 × 384 (A); 640 × 640 (B); 896 × 896 (C); 1152 × 1152 (D); and 1408 × 1408 (E) image areas. These variables showed a significantly negative correlation in all groups ($P < .001$).

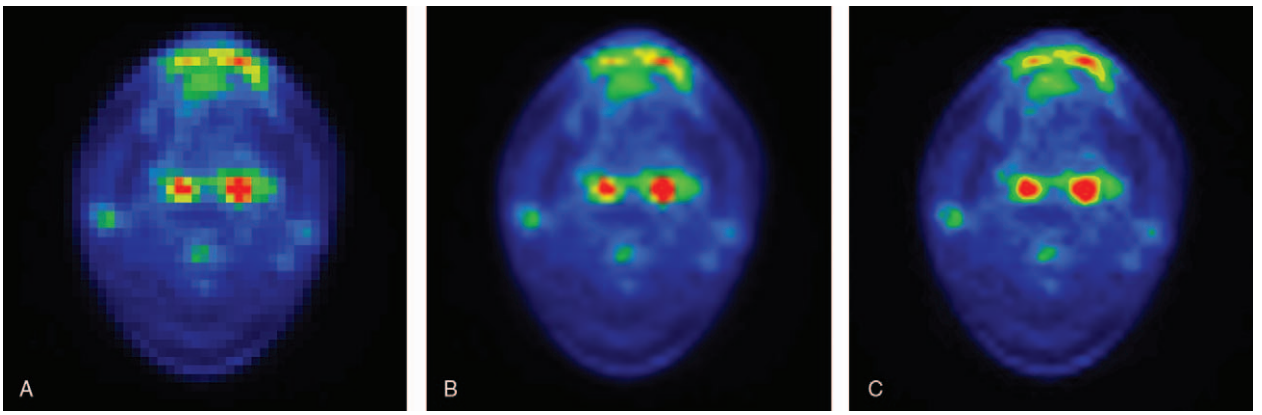

Figure 4. F-18 FDG PET original image of neck (A); high-resolution images generated by SBIM (B), and IMBIM (C) from (A). The image by SBIM was a relatively blurred, whereas the other image by IMBIM was clear and high-contrast. Detailed tracer uptake was easily identified on the IMBIM image. F-18 FDG = 2-[18F]fluoro-2-deoxyglucose, IMBIM = iterative modified bicubic interpolation method, PET = positron emission tomography, SBIM = standard bicubic interpolation method.

single photon emission CT. Establishment of high-resolution medical imaging systems which effectively diminish partial volume effect and enable better detection of small abnormalities would improve the accuracy of disease diagnosis at earlier stages, as well as their prognosis. Notably, IMBIM can be applied to all types of digital images because its algorithm is not dependent on features specific to PET images. Since digital imaging is becoming more popular world-wide, IMBIM may be expected to be used for various types of image processing technology in future.

In SBIM, weight parameters are calculated by distance, in which X and Y directions are separately computed. This calculation is advantageous for generating images with structures that have acute angles. On the other hand, some structural corners might be rounded by IMBIM. However, most structures in human PET images have no acute angle. Therefore, only distance was used to calculate weight parameters in IMBIM.

Actually, the area of each abnormal lesion is increased with IMBIM (Figs. 1 and 4). Overestimation of the area of lesion might be concerned, however, the measurement of the lesion size is usually performed on CT, not on PET. Moreover, IMBIM estimates the pixel value through multiple repeats of calculations, thereby the over-correction should be re-corrected in the next calculation, and be minimized.

Several limitations of the current study should be noted. First, this was a retrospective study limited to a single institution. In principle, IMBIM can be performed in most circumstances and does not depend on a PET/CT scanner, a tracer, patient profile, or conditions. However, multicenter randomized trials are needed to confirm the effect using IMBIM. Second, we were not able to compare high-resolution images obtained using IMBIM with real high-resolution images obtained using high-resolution hardware, such as semiconductor PET. Third, IMBIM improved contrast of image as mentioned, thereby false-positive lesion might be appeared as a result of amplified noise. But any false-positive lesion was not found in this study, because the PET images generated with IMBIM were interpreted not only on PET images but also on PET/CT fusion images, as a result, the amplified noise could be distinguished.

5. Conclusion

In conclusion, IMBIM generates high-resolution and -contrast images, which may facilitate more accurate diagnoses in clinical practice.

References

[1] Allen-Auerbach M, Weber WA. Measuring response with FDG-PET: methodological aspects. Oncologist 2009;14:369–77.
[2] De Maeseneer DJ, Lambert B, Surmont V, et al. 18-Fluorodeoxyglucose positron emission tomography as a tool for response prediction in solid tumours. Acta Clin Belg 2010;65:291–9.
[3] Nambu A, Kato S, Sato Y, et al. Relationship between maximum standardized uptake value (SUVmax) of lung cancer and lymph node metastasis on FDG-PET. Ann Nucl Med 2009;23:269–75.
[4] Yu L, Tian M, Gao X, et al. The method and efficacy of 18F-fluorodeoxyglucose positron emission tomography/computed tomography for diagnosing the lymphatic metastasis of colorectal carcinoma. Acad Radiol 2012;19:427–33.
[5] Shiono S, Abiko M, Okazaki T, et al. Positron emission tomography for predicting recurrence in stage I lung adenocarcinoma: standardized uptake value corrected by mean liver standardized uptake value. Eur J Cardiothorac Surg 2011;40:1165–9.
[6] Perez RO, Habr-Gama A, Sao Juliao GP, et al. Optimal timing for assessment of tumor response to neoadjuvant chemoradiation in patients with rectal cancer: do all patients benefit from waiting longer than 6 weeks? Int J Radiat Oncol Biol Phys 2012;84:1159–65.
[7] Fazio F, Perani D. Importance of partial-volume correction in brain PET studies. J Nucl Med 2000;41:1849–50.
[8] Meltzer CC, Kinahan PE, Greer PJ, et al. Comparative evaluation of MR-based partial-volume correction schemes for PET. J Nucl Med 1999;40:2053–65.
[9] Prieto E, Dominguez-Prado I, Garcia-Velloso MJ, et al. Impact of time-of-flight and point-spread-function in SUV quantification for oncological PET. Clin Nucl Med 2013;38:103–9.
[10] Kiyono Y, Kuge Y, Katada Y, et al. Applicability of a high-resolution small semiconductor gamma camera to small animal imaging. Nucl Med Commun 2007;28:736–41.
[11] Kubo N, Zhao S, Fujiki Y, et al. Evaluating performance of a pixel array semiconductor SPECT system for small animal imaging. Ann Nucl Med 2005;19:633–9.
[12] Shiga T, Morimoto Y, Kubo N, et al. A new PET scanner with semiconductor detectors enables better identification of intratumoral inhomogeneity. J Nucl Med 2009;50:148–55.
[13] Gao S, Gruev V. Bilinear and bicubic interpolation methods for division of focal plane polarimeters. Opt Express 2011;19:26161–73.
[14] Takei T, Shiga T, Morimoto Y, et al. A novel PET scanner with semiconductor detectors may improve diagnostic accuracy in the metastatic survey of head and neck cancer patients. Ann Nucl Med 2013;27:17–24.
[15] Usmanij EA, de Geus-Oei LF, Troost EG, et al. 18F-FDG PET early response evaluation of locally advanced non-small cell lung cancer treated with concomitant chemoradiotherapy. J Nucl Med 2013;54:1528–34.
[16] Biehl KJ, Kong FM, Dehdashti F, et al. 18F-FDG PET definition of gross tumor volume for radiotherapy of non-small cell lung cancer: is a single

standardized uptake value threshold approach appropriate? J Nucl Med 2006;47:1808–12.
[17] Calais J, Dubray B, Nkhali L, et al. High FDG uptake areas on pre-radiotherapy PET/CT identify preferential sites of local relapse after chemoradiotherapy for locally advanced oesophageal cancer. Eur J Nucl Med Mol Imaging 2015;42:858–67.
[18] Dibble EH, Alvarez AC, Truong MT, et al. 18F-FDG metabolic tumor volume and total glycolytic activity of oral cavity and oropharyngeal squamous cell cancer: adding value to clinical staging. J Nucl Med 2012;53:709–15.
[19] Werner-Wasik M, Nelson AD, Choi W, et al. What is the best way to contour lung tumors on PET scans? Multiobserver validation of a gradient-based method using a NSCLC digital PET phantom. Int J Radiat Oncol Biol Phys 2012;82:1164–71.
[20] Bonelli FS, Hartman TE, Swensen SJ, et al. Accuracy of high-resolution CT in diagnosing lung diseases. AJR Am J Roentgenol 1998;170: 1507–12.
[21] Takashima S, Maruyama Y, Hasegawa M, et al. Prognostic significance of high-resolution CT findings in small peripheral adenocarcinoma of the lung: a retrospective study on 64 patients. Lung Cancer 2002;36:289–95.